HHS Public Access

Author manuscript

Obesity (Silver Spring). Author manuscript; available in PMC 2020 August 01.

Published in final edited form as:

Obesity (Silver Spring). 2019 August ; 27(8): 1305–1313. doi:10.1002/oby.22534.

Dietary Methionine Restriction Reduces Inflammation Independent of FGF21 Action

Shaligram Sharma[1], **Taylor Dixon**[1], **Sean Jung**[1], **Emily C. Graff**[2], **Laura A. Forney**[3], **Thomas W. Gettys**[3], **Desiree Wanders**[1]

[1]Department of Nutrition, Georgia State University, Atlanta, GA, USA

[2]Department of Pathobiology, Auburn University, Auburn, AL, USA

[3]Laboratory of Nutrient Sensing and Adipocyte Signaling, Pennington Biomedical Research Center, Baton Rouge, LA, USA

Abstract

Objective: Methionine restriction (MR) decreases inflammation and improves markers of metabolic disease in rodents. MR also increases hepatic and circulating concentrations of FGF21. Emerging evidence suggests that FGF21 exerts anti-inflammatory effects. The purpose of this study was to determine the role of FGF21 in mediating the MR-induced reduction in inflammation.

Methods: Wild-type (WT) and *Fgf21*$^{-/-}$ mice were fed a high-fat (HF) control or HF MR diet for 8 weeks. In a separate experiment, mice were fed a HF diet (HFD) for 10 weeks. Vehicle or recombinant FGF21 (13.6 μg/day) were administered via osmotic minipump for an additional two weeks. Inflammation and metabolic parameters were measured.

Results: *Fgf21*$^{-/-}$ mice were more susceptible to HFD-induced inflammation, and MR reduced inflammation in white adipose tissue (WAT) and liver of *Fgf21*$^{-/-}$ mice. MR downregulated STAT3 activity in WAT of both genotypes. FGF21 administration reduced hepatic lipids and blood glucose concentrations. However, there was little effect of FGF21 on inflammatory gene expression in liver or adipose or circulating cytokines.

Conclusions: MR reduces inflammation independent of FGF21 action. Endogenous FGF21 is important to protect against the development of HFD-induced inflammation in liver and WAT, yet administration of low-dose FGF21 has little effect on markers of inflammation.

Keywords

inflammation; obesity; amino acid; FGF21; methionine

Corresponding Author Information: Desiree Wanders, Ph.D., PO Box 3995, Atlanta, GA 30302-3995, dwanders@gsu.edu.

Disclosures: No potential conflicts of interest relevant to this article were reported.

Introduction

Obesity increases adipose tissue inflammation by increasing inflammatory cytokine and chemokine production from adipocytes and resident immune cells (1) and increasing the number of inflammatory M1 macrophages present in adipose tissue (2), while reducing the presence of anti-inflammatory M2 macrophages (3). Because many inflammatory cytokines produced in adipose tissue increase insulin resistance, the elevated inflammatory state of adipose tissue provides a mechanism for the well-established link between obesity and insulin resistance (4, 5). The hepatic inflammatory response to obesity is accentuated by activation of resident Kupffer cells and chemoattraction of nonresident macrophages (6). The obesity-induced hepatic inflammation is associated with increased hepatic triglyceride stores and decreased hepatic insulin sensitivity (6).

A goal of researchers has been to identify safe and effective treatments for obesity and its comorbidities. Restriction of the essential amino acid, methionine, by 80% of normal intake reduces body weight and adiposity, improves insulin sensitivity, and reduces inflammation in rodents, despite increasing food intake (7). We have shown that dietary MR reduces age- and obesity-associated inflammation of liver and visceral and subcutaneous white adipose tissue (WAT) (8, 9), likely contributing to the improved health outcomes seen with MR. Despite producing similar reductions in body weight and adiposity, MR had a significantly greater effect on inflammatory pathways than 40% calorie restriction, and the transcriptional responses were primarily anti-inflammatory (8).

Subsequent microarray analyses of rats fed a control diet or a MR diet for 20 months identified that the MR-induced reduction in adipose tissue inflammation is likely due to upstream inhibition of signal transducer and activator of transcription 3 (STAT3) signaling in WAT (9). STAT3 is a transcription factor that, in response to cytokines and growth factors, becomes activated through phosphorylation on Tyr705 and promotes expression of several genes associated with inflammation (10). Our microarray analyses showed that 40 of the 46 target genes predicted to be activated by STAT3 were down-regulated by MR, and four of the eight genes predicted to be inhibited by STAT3 were upregulated by MR in inguinal WAT (9). Thus, the evidence is compelling that MR leads to inhibition of STAT3 signaling in WAT.

We have recently shown that MR produces a rapid and persistent increase in hepatic expression and circulating concentrations of fibroblast growth factor 21 (FGF21), and that FGF21 is an essential factor mediating the ability of MR to increase insulin sensitivity (11). Emerging evidence also suggests that FGF21 may have anti-inflammatory properties (12–15). While these studies support the idea that FGF21 exerts protective effects against inflammation, it is unclear whether FGF21 can reduce obesity-induced inflammation in adipose tissue and liver. Similarly, it has not been established whether the MR-dependent increases in FGF21 mediate the anti-inflammatory effects of dietary methionine restriction.

Methods

Animals and Diets

Experiment #1.—*Fgf21*$^{-/-}$ mice on the C57BL/6J genetic background were provided by Dr. Steven Kliewer (UT Southwestern). High-fat control (HFD) and high-fat MR (HFD + MR) diets were manufactured by Dyets Inc. (Bethlehem, PA). The energy density of the HFD and HFD + MR diets was 22.8 kJ/g, with 59.6% of energy from fat, 25.7% from carbohydrate, and 14.7% from L-amino acids. The HFD diet contained 0.86% methionine, and the HFD + MR diet contained 0.17% methionine, and neither diet contained cysteine. Male wild-type (WT; n = 24) and *Fgf21*$^{-/-}$ (n = 24) mice aged 12 wks were acclimated to the HFD diet for 4 weeks before half of the mice of each genotype were switched to the HFD + MR diet for an additional 8 weeks. Food and water were provided *ad libitum*. Mice were fasted for four hours prior to being euthanized by decapitation following CO_2-induced narcosis. Animal experiments were reviewed and approved by the Pennington Biomedical Research Center Institutional Animal Care and Use Committee (IACUC).

Experiment #2.—Five-week-old male C57BL/6J mice (n=20) were purchased from The Jackson Laboratory (Bar Harbor, ME). Mice were fed a high-fat diet with 60% of kcal derived from fat (Research Diets, Inc. #D12492, New Brunswick, NJ) for 10 weeks. After 10 weeks on the diets, mice had ALZET osmotic minipumps (DURECT Corporation, Cupertino, CA) subcutaneously implanted on the back, slightly posterior to scapulae. Minipumps delivered either vehicle (saline; n=10) or FGF21 (13.6 μg/mouse/day; n=10) subcutaneously for 14 days. Recombinant human FGF21 was purchased from R&D Systems (# 2539-FG; Minneapolis, MN). Food and water were provided *ad libitum*. Mice were fasted for four hours prior to being euthanized by decapitation following CO_2-induced narcosis. Animal experiments were reviewed and approved by the Georgia State University IACUC.

Cell Culture Studies

To assess the direct effects of MR on STAT3 phosphorylation, an established *in vitro* model (16) of MR was used. Briefly, for the experiment, HepG2 cells were treated with normal or methionine-restricted DMEM without FBS but with L-glutamine and penicillin/streptomycin. Normal DMEM contains 0.2 mM methionine and L-cystine, whereas the MR medium contains only 0.01 mM of each. After 19 hours, the cells were incubated with recombinant human IL-6 (20 ng/mL) (R&D Systems) for 30 minutes followed by measurement of phospho- and total STAT3 and SOCS3 protein expression.

Serum Analysis

Blood glucose was measured via tail nick using a One Touch Ultra Smart Glucometer following a four-hour fast just prior to sacrifice. Following decapitation, trunk blood was collected and processed for serum. Serum alanine aminotransferase (ALT), aspartate transaminase (AST), and lactate dehydrogenase 2 (LDH) concentrations were measured using a colorimetric enzymatic assay established and validated on the C311 biochemistry analyzer (Roche, Indianapolis, IN) at the Auburn University Clinical Pathology Laboratory according to standard laboratory protocol. Serum inflammatory cytokine concentrations

were measured via Luminex analysis conducted by the University of Massachusetts Medical School National Mouse Metabolic Phenotyping Center.

RNA Isolation and Quantitative Real-Time PCR

Total RNA was isolated using an RNeasy Mini Kit for liver or RNeasy Mini Lipid Tissue Kit for adipose tissue (QIAGEN Inc., Valencia, CA). One microgram of total RNA was reverse transcribed to produce cDNA. Gene expression was measured by real-time PCR (StepOne Real-Time PCR; ThermoFisher Scientific, Waltham MA) by measurement of SYBR Green. mRNA concentrations were normalized to cyclophilin expression. Primer sequences are listed in Table 1.

Histological Analysis

Liver and epididymal white adipose tissue (EWAT) were collected and stored in 10% neutral-buffered formalin for 24 hours to allow for adequate fixation. Paraffin-embedded sections were stained with hematoxylin and eosin (H&E) and examined in a blinded fashion by a board-certified veterinary pathologist (Dr. Emily Graff). For liver histological analysis, a component based and general non-alcoholic fatty liver disease (NAFLD) score was assigned based on previously published and validated criteria for rodents (17). A cumulative non-alcoholic steatohepatitis (NASH) score was calculated for each liver biopsy based on the sum of scores for micro- and macrosteatosis, hypertrophy, and inflammation. Full methods are provided in Supplemental File. For EWAT histological analysis, crown-like structures were defined as shrunken adipocytes completely surrounded by morphologically identified macrophages (18) and were counted on H&E-stained slides. The entire surface area of each fat pad was counted to provide a total number of crown-like structures per fat pad. Adipocyte area was determined as previously described (19).

Western Blot Analysis

Measurements of STAT3 phosphorylation and SOCS3 expression were obtained by Western blot analysis. Tissues were homogenized and cells were incubated in RIPA buffer containing protease and phosphatase inhibitors, aspirated four times with a 20-gauge needle, and centrifuged at 13,000 RPM for 20 minutes. Total protein concentrations in the extracts were measured by DC protein assay, SDS-PAGE was performed, and proteins were transferred to polyvinylidene fluoride membranes. Blots were probed with anti-phospho-STAT3^{Y705} (Cell Signaling Technology; Danvers, MA), total STAT3 (Santa Cruz Biotechnology; Dallas, TX), SOCS3 (Cell Signaling Technology), and β-actin (Sigma-Aldrich; St. Louis, MO). Intensity of the visualized bands was quantified by scanning densitometry using ImageJ software.

Statistical Analysis

Statistical analyses were conducted using GraphPad Prism (San Diego, CA) version 8.0.2. Data from Experiment #1 were analyzed using a two-way ANOVA with genotype and diet as main effects followed by Tukey's multiple comparison's test. Data from Experiment #2 and cell culture studies were analyzed using an unpaired t-test.

Results

Fgf21$^{-/-}$ mice are more susceptible to HFD-induced inflammation, and MR reduces inflammation in an FGF21-independent manner.

Experiment #1.—Despite having comparable body weights to the WT mice fed the HFD upon completion of the study (Fig. 1B), the *Fgf21*$^{-/-}$ mice fed the HFD had higher expression levels of inflammatory markers in liver (*Ccl2* (p=0.0007), *Adgre1* (p=0.025), *Itgam* (p=0.0099), *Itgax* (p=0.0080)) and EWAT (*Adgre1* (p=0.034) and *Itgam* (p=0.029)) than WT mice (Fig. 2), indicating that the lack of FGF21 enhances susceptibility to obesity-induced inflammation. MR produced comparable reductions in body weight in WT (44.1 g vs 27.3 g; P<0.0001) and *Fgf21*$^{-/-}$ mice (41.8 g vs 22.4 g; P<0.0001) (Fig. 1B), albeit through different mechanisms. For example, MR reduced body weight in WT mice by 40% (Fig. 1B) despite producing a 30% increase in energy intake (P<0.0001; Fig. 1C). This was due to an MR-induced increase in energy expenditure (11). In contrast, MR reduced body weight in *Fgf21*$^{-/-}$ mice (Fig. 1B) solely by reducing energy intake (P=0.037; Fig. 1C), and produced no change in energy expenditure in these mice (11). Nevertheless, MR reduced inflammatory gene expression in liver and EWAT of *Fgf21*$^{-/-}$ mice (Fig. 2), indicating that FGF21 was not necessary to mediate the anti-inflammatory effects of MR. Specifically, in the *Fgf21*$^{-/-}$ mice, MR reduced expression of *Ccl2* (P<0.0001), *Itgam* (P=0.007), and *Itgax* (P=0.009) in the liver and reduced expression of *Ccl2* (P=0.006), *Adgre1* (P=0.0005), *Itgam* (P=0.022), and *Itgax* (P=0.004) in EWAT. MR significantly reduced expression of *Ccl2* in EWAT of WT mice (P=0.0002) but had no significant effect on other inflammatory markers that were measured (Fig. 2). Lastly, it should be noted that expression of inflammatory markers in liver and EWAT did not differ between genotypes in mice fed the HFD + MR.

Methionine restriction downregulates STAT3 signaling.

Given the documented association of STAT3 with pro-inflammatory responses (10, 20–22), we aimed to determine whether the ability of MR to reduce inflammation in these tissues is mediated by a reduction in STAT3 activity. In Experiment #1, we measured STAT3 phosphorylation at tyrosine 705 as an indicator of its activity state. MR downregulated STAT3 phosphorylation in EWAT of WT (P=0.010) and *Fgf21*$^{-/-}$ (P<0.0001) mice (Fig. 3A and 3B), suggesting that the proinflammatory transcription factor may be the mechanism mediating the MR-induced downregulation of inflammatory markers. Although these findings are consistent with our bioinformatic prediction of STAT3 activation in WAT, MR did not significantly downregulate STAT3 signaling in the liver of either genotype (P>0.19) (Fig. 3C and 3D). Interestingly, the reduction of media methionine prevented the IL-6-induced increase in STAT3 signaling in HepG2 cells (P=0.017) (Fig. 3E and 3F). These cell-autonomous effects indicate that the ability of MR to downregulate STAT3 signaling is direct and independent of weight loss. MR also increased SOCS3 expression in HepG2 cells (P=0.0497) (Fig. 3G and 3H). SOCS3 acts in a negative feedback manner to inhibit STAT3 activity (23).

Pharmacologic administration of FGF21 reduces blood glucose concentrations and hepatic steatosis but has no effect on inflammatory markers.

The marked susceptibility of *Fgf21*$^{-/-}$ mice to HFD-induced inflammation (Fig. 2)suggests that FGF21 exerts protective effects against HFD-induced inflammation. To test whether pharmacologic administration of low-dose FGF21 could reverse obesity-induced inflammation, in Experiment #2, mice were fed a HFD for 10 weeks and then were subcutaneously administered vehicle or recombinant FGF21 (13.6 μg/mouse/day) for an additional two weeks. Vehicle- and FGF21-treated mice had similar body weights at the time of minipump implantation (Fig. 4A). During the two weeks of FGF21 administration, the main effect of FGF21 to lower body weight was significant (P=0.026), with final body weights of the FGF21-treated mice trending (P=0.073) to be reduced (Fig. 4A). FGF21 administration reduced fasting blood glucose concentrations (P=0.0397; Fig. 4B) and histologically-observed hepatic steatosis (Fig. 4C). Specifically, FGF21-treated mice had significantly decreased microsteatosis (P=0.0131) and overall NASH score (P=0.041; Fig. 4D–G), with no effects on macrosteatosis (P=0.5560) and hypertrophy (P=0.135). Histologically-observed inflammation was not present in livers of vehicle- or FGF21-treated mice. Together, these data suggest that FGF21 treatment produced a mild, but significant decrease in hepatic lipid content (Fig. 4C–G).

Despite producing expected reductions in blood glucose concentrations and hepatic lipids, FGF21 had no effect on gene expression of inflammatory markers in liver (Fig. 5A–E) or EWAT (Fig. 6C–H). FGF21 treatment had no effect on expression of *Adgre1* (P=0.59; Fig. 5A), *Itgax* (P=0.93; Fig. 5B), *Itgam* (P=0.37; Fig. 5C), *Ccl2* (P=0.07; Fig. 5D), and *Il1b* (P=0.22; Fig. 5E) in the liver. To further examine the effects of FGF21 on hepatic injury, serum concentrations of AST, ALT, and LDH were measured. While all three markers of live injury trended down in the FGF21-treated mice, FGF21 had no significant effect on serum AST (P=0.08), ALT (P=0.09), or LDH (P=0.07) (Fig. 5F–H) concentrations. Two weeks of FGF21 administration had no significant effects on the presence of crown-like structures in the EWAT (Fig. 6A&B). Like the liver, FGF21 treatment had no effect on expression of *Adgre1* (P=0.50; Fig. 5C), *Itgax* (P=0.51; Fig. 5D), *Itgam* (P=0.78; Fig. 5E), *Ccl2* (P=0.62; Fig. 5F), *Il6* (P=0.85; Fig. 5G) and *Il1b* (P=0.09; Fig. 5H) in the EWAT. Consistent with a lack of effect of FGF21 on inflammatory markers in liver and EWAT, FGF21 had no effect on the cytokines, MCP-1 (0.46) and TNF-α (0.58), in the serum (Fig. 7). FGF21 reduced IL-6 concentrations in the serum by 40%, but this did not reach statistical significance (P=0.17).

Discussion

One goal of these studies was to determine whether FGF21 was an important mediator of the anti-inflammatory effects of MR. To this aim, WT and *Fgf21*$^{-/-}$ mice were fed a HFD for 4 weeks prior to half of the mice being switched to a HF MR diet for an additional 8 weeks. Despite having similar weights to the WT mice at the end of the experiment, *Fgf21*$^{-/-}$ mice had higher levels of inflammation in liver and adipose tissue. *Fgf21*$^{-/-}$ mice fed a HFD for 12 weeks had higher expression of the genes that encode the proteins F4/80, CD11b, and CD11c in EWAT and liver. Along with these changes, the liver also had greater expression of

the gene that encodes for MCP-1 (Fig. 2). CD11c-expressing macrophages are recruited to tissues, like adipose and muscle, during obesity and release high levels of pro-inflammatory cytokines that contribute to the development of insulin resistance (24). In fact, macrophages that express F4/80, CD11b, and CD11c represent a specific population of macrophages that are recruited to adipose tissue in response to HFD feeding (24). The greater expression of these genes indicates that *Fgf21*$^{-/-}$ mice were not only more susceptible to HFD-induced inflammation but were also likely at greater risk for insulin resistance. Indeed, *Fgf21*$^{-/-}$ mice have been shown to have greater adipose tissue inflammation and insulin resistance compared to WT mice (25). Similarly, others have shown that *Fgf21*$^{-/-}$ mice have elevated levels of inflammation in pancreas when fed a HFD (14) compared to WT mice. Interestingly, while we found that *Fgf21*$^{-/-}$ mice had greater hepatic inflammation compared to WT mice fed a HFD for 12 weeks, a longer-term study found no difference in hepatic inflammation between WT and *Fgf21*$^{-/-}$ mice fed a high-fat, high-sucrose diet for 52 weeks (26). The increased expression of inflammatory markers in the liver of *Fgf21*$^{-/-}$ mice may be due to activation of resident liver macrophages (Kupffer cells) or hepatic infiltration by newly recruited immune cells, both of which occur in obesity (27, 28). Likewise, the increased expression of inflammatory markers in adipose tissue of *Fgf21*$^{-/-}$ mice may be due to increased cytokine expression by adipocytes themselves, but is more likely due to an increased presence of inflammatory immune cells (1, 2). One limitation of this study is the lack of flow cytometric analysis to identify the number and type of immune cells present in the liver and EWAT.

Despite emerging evidence that FGF21 exerts anti-inflammatory effects, we report for the first time that the lack of FGF21 did not hinder the ability of MR to reduce inflammation. MR significantly reduced expression of *Ccl2, Itgam,* and *Itgax* in liver and *Ccl2, Adgre1, Itgam,* and *Itgax* in adipose tissue of *Fgf21*$^{-/-}$ mice (Fig. 2). These findings are in line with a previous study that reported that although exercise both increases FGF21 and reduces inflammation, FGF21 is not required for the exercise-induced reduction in inflammation in adipose tissue (25). As previously reported (11), MR produced an unexpected reduction in food intake in *Fgf21*$^{-/-}$ mice. Despite not increasing energy expenditure in the *Fgf21*$^{-/-}$ mice, MR still reduced body weight due to the reduction in food intake. The MR-induced reduction in food intake and body weight in the *Fgf21*$^{-/-}$ mice may play a role in reducing expression of inflammatory markers in this group.

Our current findings that some effects of MR are independent of FGF21 is consistent with a previous report that demonstrated that methionine deprivation induced similar metabolic effects in male and female mice, despite increasing plasma FGF21 in males only (29). Similarly, additional studies reported FGF21-dependent and -independent responses to metabolic stress and cold stress (30, 31). Collectively, these findings suggest that the role of FGF21 in dietary methionine restriction and the stress response is complex and requires further investigation.

Somewhat surprisingly, MR did not significantly affect many of the inflammatory markers measured in liver or EWAT of WT mice. This may be due to the low levels of inflammation in the tissues of the WT mice. Some studies have shown that 12 weeks of HFD feeding may not be long enough to produce significant increases in inflammation, especially in the liver

(32), while other studies have reported HFD-induced increases in adipose tissue inflammation after just three days (33). Our previous studies showing that MR reduces inflammation in liver and subcutaneous and visceral WAT in rodents used significantly longer time frames. For example, we showed that MR reduced age-associated inflammation in liver, retroperitoneal WAT, epididymal WAT, and inguinal WAT of rats fed the diet for 20 months (8) and that MR reduced obesity-associated hepatic inflammation in obesity-prone Osborne Mendel rats fed the diet for 7 months (8). These longer timeframes allowed for the development of age- and obesity-induced inflammation that was present at a lower magnitude in the WT mice of Experiment #1. It may be that MR was effective at reducing inflammation in the *Fgf21*$^{-/-}$ mice due to their elevated levels of inflammation but had no effect in the WT mice because of their already low levels of inflammation.

The coordinated downregulation of inflammatory genes known to be regulated by STAT3 suggests that the MR-dependent anti-inflammatory responses in WAT are being mediated by MR-dependent inhibition of STAT3 activity (9). Another group used microarray analyses and found that MR also downregulates STAT3 signaling in the liver of a mouse model of Hutchinson-Gilford progeria syndrome (34). To determine whether MR affects STAT3 activity, we measured STAT3 phosphorylation in liver and EWAT of WT and *Fgf21*$^{-/-}$ mice fed HFD or HFD + MR for 8 weeks (Fig. 3). In adipose tissue, *Fgf21*$^{-/-}$ mice had elevated STAT3 activity compared to WT mice, but MR produced comparable reductions in STAT3 phosphorylation in both genotypes. These novel data suggest that the MR-induced reduction in STAT3 signaling may be responsible for the subsequent reduction in inflammation. The mechanism by which MR regulates STAT3 phosphorylation in adipose tissue remains unknown. However, it is well documented that dietary MR reduces circulating and adipose tissue leptin concentrations (35) and leptin is a potent activator of STAT3 in adipose tissue (36). Therefore, dietary MR may reduce adipose tissue STAT3 phosphorylation via reduced adipose tissue or circulating leptin concentrations. There were no significant effects of genotype or diet on STAT3 signaling in the liver. While reduced STAT3 signaling may be responsible for the reduction in inflammation in the adipose tissue, another mechanism seems likely for the reduced hepatic inflammation. We previously reported that these *Fgf21*$^{-/-}$ mice have elevated hepatic triglycerides and that MR reduces hepatic triglycerides in both WT and *Fgf21*$^{-/-}$ mice (11). Elevated hepatic lipid accumulation is strongly linked to hepatic inflammation (37). The changes in hepatic lipids seen in response to the lack of FGF21 and to the MR diet may explain the changes in hepatic inflammation. While we did not see significant effects of MR on hepatic STAT3 activity, *in vivo*, *in vitro* methionine restriction suppressed IL-6-induced STAT3 phosphorylation in HepG2 cells (Fig. 3). These cell-autonomous effects indicate that the ability of MR to downregulate STAT3 signaling is direct and independent of weight loss or reduced leptin. At the same time, MR increased expression of SOCS3 in HepG2 cells, which negatively feeds back to inhibit STAT3 activity (23).

Because of the marked susceptibility of *Fgf21*$^{-/-}$ mice to HFD-induced inflammation, it was evident that FGF21 exerts protective effects against HFD-induced inflammation. It has been well-established that pharmacologic levels of FGF21, achieved either through exogenous administration of FGF21 or overexpression of FGF21, result in reduced body weight, blood glucose concentrations, and hepatic lipids in mice (38). Thus, the FGF21-induced reductions

in blood glucose concentrations and significant improvements in histologically observed hepatic steatosis after two weeks of FGF21 administration were in line with previous reports. Consistent with the mild changes noted in the liver histopathology induced by FGF21, FGF21 treatment slightly, but not significantly reduced serum AST (P=0.08), ALT (P=0.09), and LDH (P=0.07) concentrations. Elevations in serum AST, ALT, and LDH are typical with high-fat diet-induced obesity and are indicative of hepatocellular damage. While not explored in this study, previous reports have identified that FGF21 reduces hepatic lipids by reducing expression of genes associated with hepatic de novo lipogenesis (39) and increasing hepatic lipid oxidation (40) and hepatic expression of genes associated with lipid oxidation (41). Others have shown that the FGF21-induced reduction in hepatic triglycerides is due to FGF21 action on adipocytes, limiting the fatty acid supply and triglyceride content in liver (42).

A growing body of literature in cell culture and animal models indicates that FGF21 possesses anti-inflammatory properties (12–15, 43, 44). One recent study demonstrated that *Fgf21*$^{-/-}$ mice fed a high-fat diet had a lower number of anti-inflammatory M2 macrophages in inguinal WAT compared to WT mice, but that replenishing FGF21 to normal levels increased the number of M2 (anti-inflammatory) macrophages without changing the number of M1 (pro-inflammatory) macrophages (15). In our study, FGF21 treatment had no effect on markers of M1 macrophages in liver or EWAT (Fig. 5 and Fig. 6). Similarly, mRNA expression of M2 macrophages in these tissues did not change following FGF21 treatment (data not shown). The lack of effect of FGF21 on markers of inflammation was most likely due to the low-dose and/or short duration of FGF21 used in this study. Though the number of published studies are limited, other studies demonstrating anti-inflammatory effects of exogenous FGF21 in adipose tissue or liver of different animal models of inflammation used 3–13 times the dose that was used in this study (43, 45) or used higher doses of a long-acting FGF21 analog (12) and often used longer treatment durations. The duration of two-weeks of FGF21 administration was studied because we aimed to see whether FGF21 treatment itself produced any anti-inflammatory responses prior to the expected FGF21-induced reduction in body weight. Inclusion of a chow or low-fat control diet group would have been useful to serve as a reference point for the amount of change in inflammatory markers and hepatic lipids. Considered together, the presence of inflammation in the mice was mild and was variable between the mice.

Future studies including female mice will provide more thorough insight into the mechanism of action of the MR diet and FGF21 and will enhance the translational potential of the findings. Additionally, it is possible that constitutive deletion of FGF21 may have resulted in some developmental changes in the mice. Future studies should include the use of inducible *Fgf21* knockout.

Conclusions

MR reduces inflammation in liver and EWAT independent of FGF21 action. Endogenous FGF21 is important to protect against the development of high-fat diet-induced inflammation of liver and EWAT, yet pharmacologic administration of low-dose FGF21 for two weeks has no effect on markers of inflammation in mice.

Supplementary Material

Refer to Web version on PubMed Central for supplementary material.

Acknowledgments

Funding: This work was supported in part by the Center for Obesity Reversal at Georgia State University seed grant (D.W.), the American Diabetes Association grant 1-12-BS-58 (T.W.G.), National Institute of Diabetes and Digestive and Kidney Diseases grant NIH R01-DK-096311 (T.W.G.) L.A.F. was supported by an American Diabetes Association mentor-based postdoctoral fellowship (7-13-MI-05). Part of this study was conducted at the National Mouse Metabolic Phenotyping Center (MMPC) at the University of Massachusetts Medical School and supported by NIH grant 5U2C-DK093000-07.

REFERENCES

1. Fain JN. Release of interleukins and other inflammatory cytokines by human adipose tissue is enhanced in obesity and primarily due to the nonfat cells. Vitam Horm 2006;74:443–477. [PubMed: 17027526]
2. Weisberg SP, McCann D, Desai M, Rosenbaum M, Leibel RL, Ferrante AW Jr. Obesity is associated with macrophage accumulation in adipose tissue. J Clin Invest 2003;112:1796–1808. [PubMed: 14679176]
3. Lumeng CN, Bodzin JL, Saltiel AR. Obesity induces a phenotypic switch in adipose tissue macrophage polarization. J Clin Invest 2007;117:175–184. [PubMed: 17200717]
4. Duval C, Thissen U, Keshtkar S, et al. Adipose tissue dysfunction signals progression of hepatic steatosis towards nonalcoholic steatohepatitis in c57bl/6 mice. Diabetes 2010;59:3181–3191. [PubMed: 20858684]
5. Lazar MA. How obesity causes diabetes: Not a tall tale. Science 2005;307:373–375. [PubMed: 15662001]
6. Lackey DE, Olefsky JM. Regulation of metabolism by the innate immune system. Nat Rev Endocrinol 2016;12:15–28. [PubMed: 26553134]
7. Orgeron ML, Stone KP, Wanders D, Cortez CC, Van NT, Gettys TW. The impact of dietary methionine restriction on biomarkers of metabolic health. Prog Mol Biol Transl Sci 2014;121:351–376. [PubMed: 24373243]
8. Wanders D, Ghosh S, Stone KP, Van NT, Gettys TW. Transcriptional impact of dietary methionine restriction on systemic inflammation: Relevance to biomarkers of metabolic disease during aging. Biofactors 2014;40:13–26. [PubMed: 23813805]
9. Ghosh S, Wanders D, Stone KP, Van NT, Cortez CC, Gettys TW. A systems biology analysis of the unique and overlapping transcriptional responses to caloric restriction and dietary methionine restriction in rats. FASEB J 2014;28:2577–2590. [PubMed: 24571921]
10. Carpenter RL, Lo HW. Stat3 target genes relevant to human cancers. Cancers (Basel) 2014;6:897–925. [PubMed: 24743777]
11. Wanders D, Forney LA, Stone KP, Burk DH, Pierse A, Gettys TW. Fgf21 mediates the thermogenic and insulin-sensitizing effects of dietary methionine restriction but not its effects on hepatic lipid metabolism. Diabetes 2017;66:858–867. [PubMed: 28096260]
12. Talukdar S, Zhou Y, Li D, et al. A long-acting fgf21 molecule, pf-05231023, decreases body weight and improves lipid profile in non-human primates and type 2 diabetic subjects. Cell Metab 2016;23:427–440. [PubMed: 26959184]
13. Gao M, Ma Y, Cui R, Liu D. Hydrodynamic delivery of fgf21 gene alleviates obesity and fatty liver in mice fed a high-fat diet. J Control Release 2014;185:1–11. [PubMed: 24747761]
14. Singhal G, Fisher FM, Chee MJ, et al. Fibroblast growth factor 21 (fgf21) protects against high fat diet induced inflammation and islet hyperplasia in pancreas. PLoS One 2016;11:e0148252. [PubMed: 26872145]
15. Li H, Wu G, Fang Q, et al. Fibroblast growth factor 21 increases insulin sensitivity through specific expansion of subcutaneous fat. Nat Commun 2018;9:272. [PubMed: 29348470]

16. Stone KP, Wanders D, Orgeron M, Cortez CC, Gettys TW. Mechanisms of increased in vivo insulin sensitivity by dietary methionine restriction in mice. Diabetes 2014;63:3721–3733. [PubMed: 24947368]
17. Liang W, Menke AL, Driessen A, et al. Establishment of a general nafld scoring system for rodent models and comparison to human liver pathology. PLoS One 2014;9:e115922. [PubMed: 25535951]
18. Cinti S, Mitchell G, Barbatelli G, et al. Adipocyte death defines macrophage localization and function in adipose tissue of obese mice and humans. J Lipid Res 2005;46:2347–2355. [PubMed: 16150820]
19. Luo Y, Burrington CM, Graff EC, et al. Metabolic phenotype and adipose and liver features in a high-fat western diet-induced mouse model of obesity-linked nafld. Am J Physiol Endocrinol Metab 2016;310:E418–439. [PubMed: 26670487]
20. Aggarwal BB, Kunnumakkara AB, Harikumar KB, et al. Signal transducer and activator of transcription-3, inflammation, and cancer: How intimate is the relationship? Ann N Y Acad Sci 2009;1171:59–76. [PubMed: 19723038]
21. Przanowski P, Dabrowski M, Ellert-Miklaszewska A, et al. The signal transducers stat1 and stat3 and their novel target jmjd3 drive the expression of inflammatory genes in microglia. J Mol Med (Berl) 2014;92:239–254. [PubMed: 24097101]
22. Yu H, Pardoll D, Jove R. Stats in cancer inflammation and immunity: A leading role for stat3. Nat Rev Cancer 2009;9:798–809. [PubMed: 19851315]
23. Jiang M, Zhang WW, Liu P, Yu W, Liu T, Yu J. Dysregulation of socs-mediated negative feedback of cytokine signaling in carcinogenesis and its significance in cancer treatment. Front Immunol 2017;8:70. [PubMed: 28228755]
24. Patsouris D, Li PP, Thapar D, Chapman J, Olefsky JM, Neels JG. Ablation of cd11c-positive cells normalizes insulin sensitivity in obese insulin resistant animals. Cell Metab 2008;8:301–309. [PubMed: 18840360]
25. Porter JW, Rowles JL 3rd, Fletcher JA, et al. Anti-inflammatory effects of exercise training in adipose tissue do not require fgf21. J Endocrinol 2017;235:97–109. [PubMed: 28765264]
26. Singhal G, Kumar G, Chan S, et al. Deficiency of fibroblast growth factor 21 (fgf21) promotes hepatocellular carcinoma (hcc) in mice on a long term obesogenic diet. Mol Metab 2018;13:56–66. [PubMed: 29753678]
27. Mayoral Monibas R, Johnson AM, Osborn O, Traves PG, Mahata SK. Distinct hepatic macrophage populations in lean and obese mice. Front Endocrinol (Lausanne) 2016;7:152. [PubMed: 27999564]
28. Tencerova M, Aouadi M, Vangala P, et al. Activated kupffer cells inhibit insulin sensitivity in obese mice. FASEB J 2015;29:2959–2969. [PubMed: 25805830]
29. Yu D, Yang SE, Miller BR, et al. Short-term methionine deprivation improves metabolic health via sexually dimorphic, mtorc1-independent mechanisms. FASEB J 2018;32:3471–3482. [PubMed: 29401631]
30. Ost M, Coleman V, Voigt A, et al. Muscle mitochondrial stress adaptation operates independently of endogenous fgf21 action. Mol Metab 2016;5:79–90. [PubMed: 26909316]
31. Keipert S, Kutschke M, Ost M, et al. Long-term cold adaptation does not require fgf21 or ucp1. Cell Metab 2017;26:437–446 e435. [PubMed: 28768181]
32. van der Heijden RA, Sheedfar F, Morrison MC, et al. High-fat diet induced obesity primes inflammation in adipose tissue prior to liver in c57bl/6j mice. Aging (Albany NY) 2015;7:256–268. [PubMed: 25979814]
33. Lee YS, Li P, Huh JY, et al. Inflammation is necessary for long-term but not short-term high-fat diet-induced insulin resistance. Diabetes 2011;60:2474–2483. [PubMed: 21911747]
34. Barcena C, Quiros PM, Durand S, et al. Methionine restriction extends lifespan in progeroid mice and alters lipid and bile acid metabolism. Cell Rep 2018;24:2392–2403. [PubMed: 30157432]
35. Hasek BE, Stewart LK, Henagan TM, et al. Dietary methionine restriction enhances metabolic flexibility and increases uncoupled respiration in both fed and fasted states. Am J Physiol Regul Integr Comp Physiol 2010;299:R728–739. [PubMed: 20538896]

36. Bendinelli P, Maroni P, Pecori Giraldi F, Piccoletti R. Leptin activates stat3, stat1 and ap-1 in mouse adipose tissue. Mol Cell Endocrinol 2000;168:11–20. [PubMed: 11064148]

37. Gao B, Tsukamoto H. Inflammation in alcoholic and nonalcoholic fatty liver disease: Friend or foe? Gastroenterology 2016;150:1704–1709. [PubMed: 26826669]

38. Kliewer SA, Mangelsdorf DJ. A dozen years of discovery: Insights into the physiology and pharmacology of fgf21. Cell Metab 2019;29:246–253. [PubMed: 30726758]

39. Xu J, Lloyd DJ, Hale C, et al. Fibroblast growth factor 21 reverses hepatic steatosis, increases energy expenditure, and improves insulin sensitivity in diet-induced obese mice. Diabetes 2009;58:250–259. [PubMed: 18840786]

40. Camporez JP, Jornayvaz FR, Petersen MC, et al. Cellular mechanisms by which fgf21 improves insulin sensitivity in male mice. Endocrinology 2013;154:3099–3109. [PubMed: 23766126]

41. Coskun T, Bina HA, Schneider MA, et al. Fibroblast growth factor 21 corrects obesity in mice. Endocrinology 2008;149:6018–6027. [PubMed: 18687777]

42. Schlein C, Talukdar S, Heine M, et al. Fgf21 lowers plasma triglycerides by accelerating lipoprotein catabolism in white and brown adipose tissues. Cell Metab 2016;23:441–453. [PubMed: 26853749]

43. Wang WF, Li SM, Ren GP, et al. Recombinant murine fibroblast growth factor 21 ameliorates obesity-related inflammation in monosodium glutamate-induced obesity rats. Endocrine 2015;49:119–129. [PubMed: 25306889]

44. Yu Y, He J, Li S, et al. Fibroblast growth factor 21 (fgf21) inhibits macrophage-mediated inflammation by activating nrf2 and suppressing the nf-kappab signaling pathway. Int Immunopharmacol 2016;38:144–152. [PubMed: 27276443]

45. Liu Y, Zhao C, Xiao J, et al. Fibroblast growth factor 21 deficiency exacerbates chronic alcohol-induced hepatic steatosis and injury. Sci Rep 2016;6:31026. [PubMed: 27498701]

What is already known about this subject?

- Dietary methionine restriction reduces age- and obesity-associated inflammation.
- Methionine restriction increases tissue and circulating concentrations of FGF21.
- Emerging evidence suggests that FGF21 exerts anti-inflammatory effects.

What does your study add?

- Mice lacking FGF21 are more susceptible to high-fat diet-induced inflammation.
- Methionine restriction reduces inflammation independent of FGF21 effects.
- Administration of low-dose FGF21 has no effect on markers of inflammation in liver, adipose tissue, or serum.

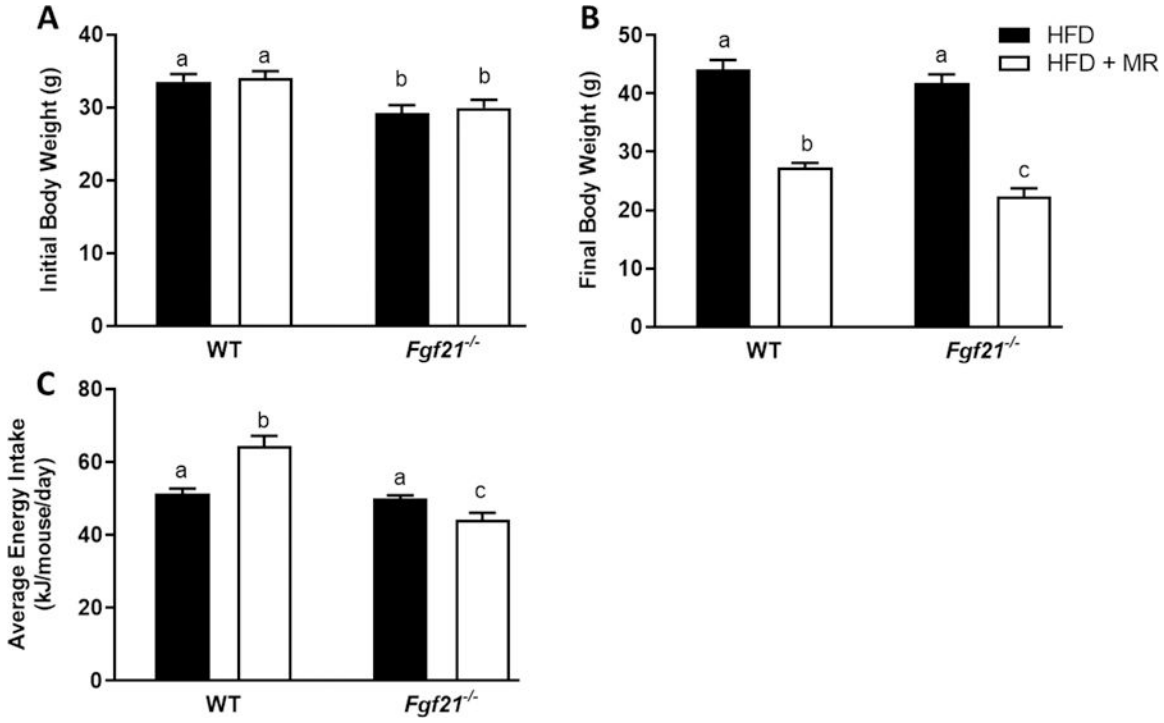

FIGURE 1. Body weight and energy intake in WT and *Fgf21*$^{-/-}$ mice fed a high-fat control (HFD) or high-fat methionine-restricted diet (HFD + MR).

Male WT and *Fgf21*$^{-/-}$ mice (12 weeks old) were fed the HFD for 4 weeks before half of the mice of each genotype were randomized to remain on the HFD and the remaining half of mice were switched to the HFD + MR for 8 weeks. Initial (A) and final (B) body weights and average energy intake (C) over the first 6 weeks of the diets are represented by means +/− SEM of 12 mice per group. Means annotated with different letters denote statistically significant differences at $P < 0.05$.

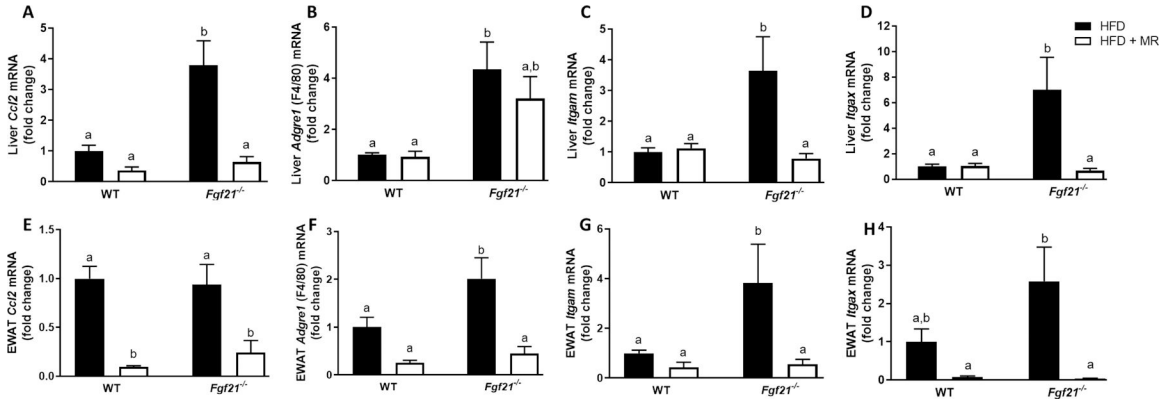

FIGURE 2. Inflammatory gene expression in liver and adipose tissue of WT and *Fgf21*$^{-/-}$ mice fed a high-fat control (HFD) or high-fat methionine-restricted diet (HFD + MR).

Male WT and *Fgf21*$^{-/-}$ mice (12 weeks old) were fed the HFD for 4 weeks before half of the mice of each genotype were randomized to remain on the HFD and the remaining half of mice were switched to the HFD + MR for 8 weeks. Effects of MR on inflammatory gene expression in liver (A-D) and EWAT (E-H) were expressed as fold change compared to the WT mice fed the HFD. The means +/− standard error are representative of 7–10 mice per group. Means annotated with different letters denote statistically significant differences at $P < 0.05$.

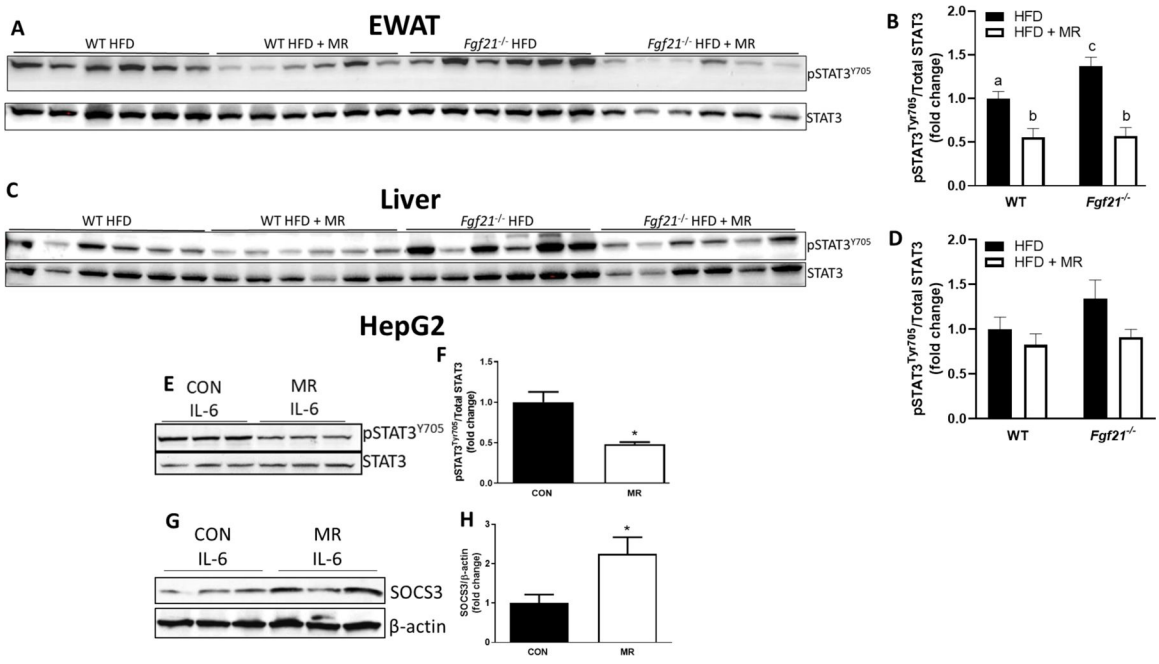

FIGURE 3. MR reduces STAT3 phosphorylation in WT and *Fgf21*$^{-/-}$ mice.

STAT3 phosphorylation in EWAT (A & B) and liver (C & D) of mice fed a HFD or HFD + MR for 8 weeks. STAT3 phosphorylation (E & F) and SOCS3 expression (G & H) in HepG2 cells that were cultured in control or MR media for 19 hours followed by IL-6 treatment (20 ng/mL) for 30 minutes. Data are expressed as means +/− SEM. Phospho-STAT3 was normalized to total STAT3. SOCS3 was normalized to β-actin. *Denotes statistically significant differences at $P < 0.05$.

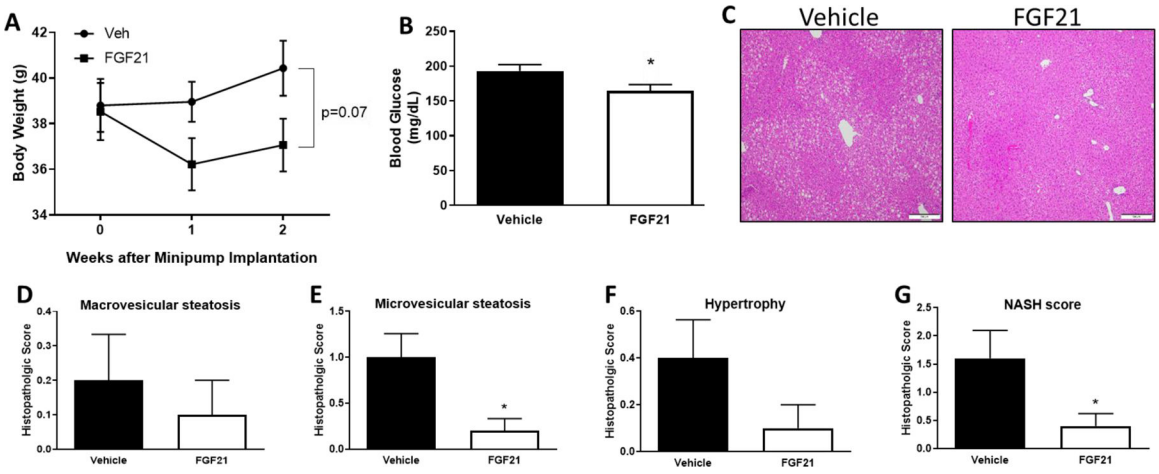

FIGURE 4. Effects of FGF21 on body weight, blood glucose concentrations, and hepatic lipids.

Male C57BL/6J mice were fed a high-fat diet for 12 weeks. Vehicle or FGF21 (13.6 μg/day) were administered via osmotic minipumps for last two weeks of the study. Body weight (A) and blood glucose concentrations (B) were measured prior to sacrifice after a 4 hour fast. Liver H&E stains (C), macrovesicular steatosis (D), microvesicular steatosis (E), hypertrophy (F), and NASH score (G) were measured as described in Methods. Data are presented as means +/− SEM for n=9–10 per group. *Denotes statistically significant differences at $P < 0.05$.

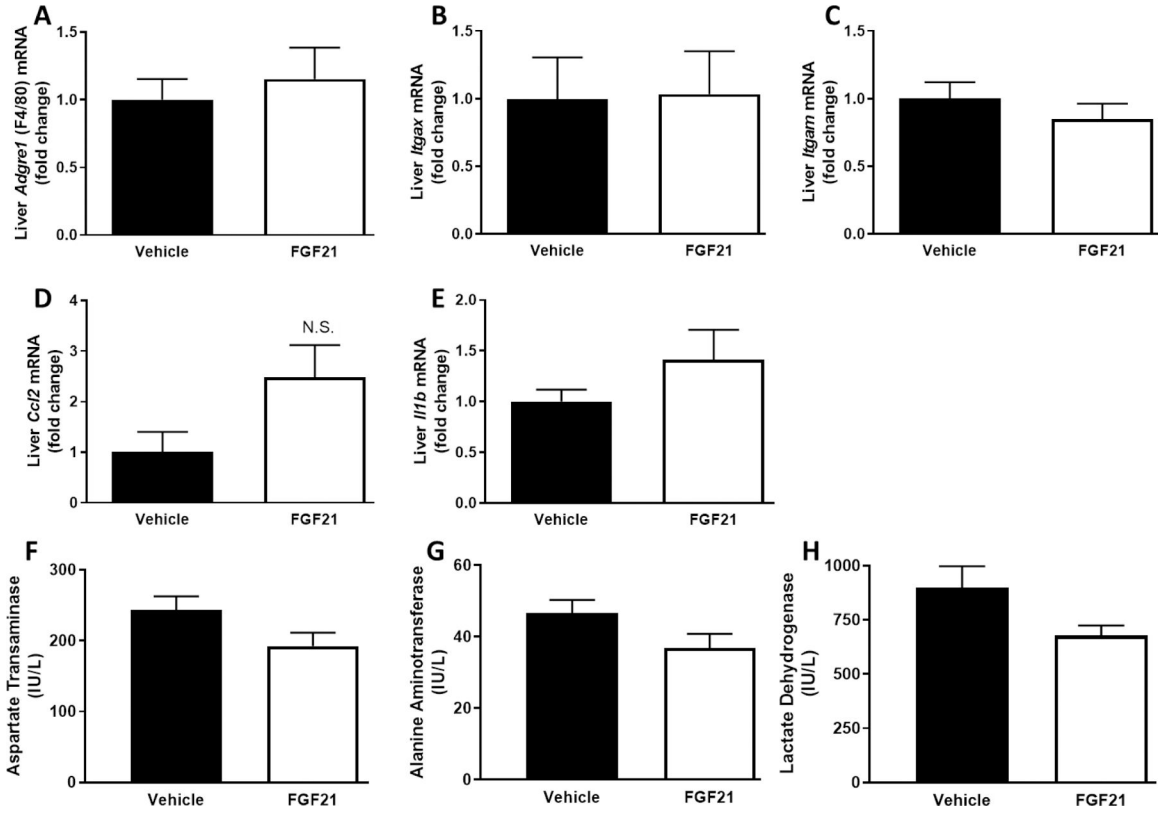

FIGURE 5. Short-term, low-dose FGF21 has no significant effect on liver inflammation or injury.

Male C57BL/6J mice were fed a high-fat diet for 12 weeks. Vehicle or FGF21 (13.6 μg/day) were administered via osmotic minipumps for last two weeks of the study. Effects of FGF21 on inflammatory gene expression in liver (A-E) were expressed as fold change compared to the vehicle-treated group. Aspartate transaminase (F), alanine aminotransferase (G), and lactate dehydrogenase (H) were measured in serum collected after a four hour fast. The means +/− SEM are representative of 7–10 mice per group. N.S.; not significant.

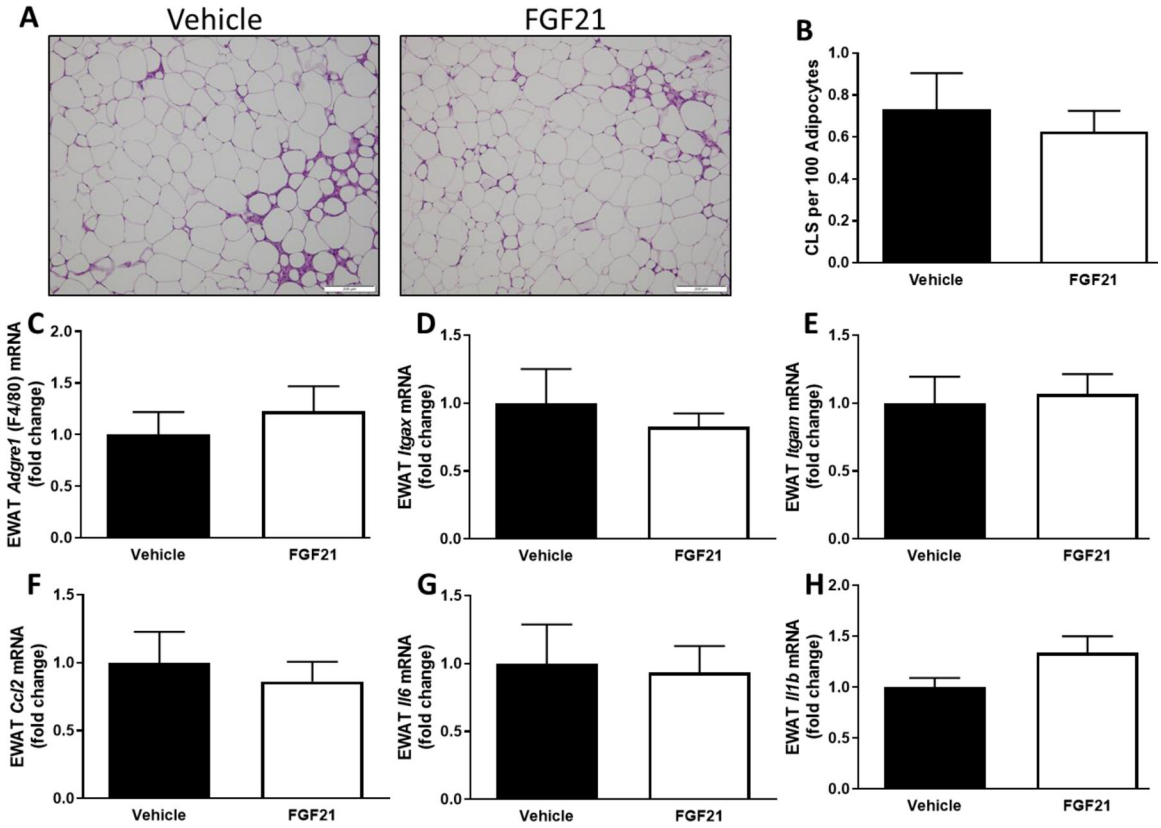

FIGURE 6. Short-term, low-dose FGF21 has no effect on adipose tissue inflammation.

Male C57BL/6J mice were fed a high-fat diet for 12 weeks. Vehicle or FGF21 (13.6 μg/day) were administered via osmotic minipumps for last two weeks of the study. Representative H&E stains of EWAT (A) and quantified number of crown-like structures (CLS) (B). Effects of FGF21 on inflammatory gene expression in EWAT (C-H) were expressed as fold change compared to the vehicle-treated group. The means +/− SEM are representative of 7–10 mice per group.

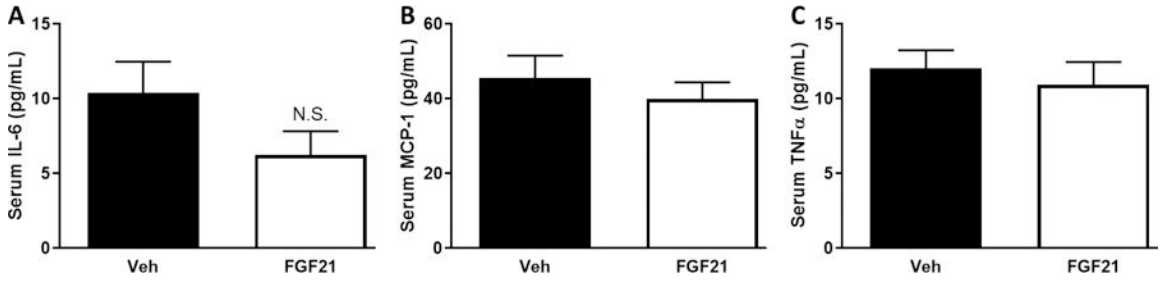

FIGURE 7. Short-term, low-dose FGF21 has no effect on circulating inflammatory markers.

Male C57BL/6J mice were fed a high-fat diet for 12 weeks. Vehicle or FGF21 (13.6 μg/day) were administered via osmotic minipumps for last two weeks of the study. Serum IL-6 (A), MCP-1 (B), and TNF-α (C) concentrations were measured by Luminex assay after a four hour fast. Data are presented as means +/− SEM for n=6–10 per group. N.S.; not significant.

Table 1.

Primer sequences used in real-time PCR.

All sequences are specific to mice, with exception of *Ppia* (cyclophilin), which is universal.

Gene	Forward Sequence	Reverse Sequence
Adgre1 (F4/80)	5'-GTG CCA TCA TTG CGG GAT TC-3'	5'-GAC GGT TGA GCA GAC AGT GA-3'
Ccl2 (MCP1)	5'-GGA GAG ACA GCG GTC GTA AG-3'	5'-CCA GCC GGC AAC TGT GA-3'
Il1b (IL-1β)	5-TGC CAC CTT TTG ACA GTG ATG-3'	5-TTC TTG TGA CCC TGA GCG AC-3'
Il6 (IL-6)	5'-ATG GAT GCT ACC AAA CTG GAT-3'	5'-TGA AGG ACT CTG GCT TTG TCT-3'
Itgam (CD11b)	5'-CCA CAC TAG CAT CAA GGG CA-3'	5'-CCC TGA TCA CCG TGG AGA AG-3'
Itgax (CD11c)	5'-GGG ACG CTT ACC TGG GTT AC-3'	5'-CCT GGA AAT CTC TGC AGG TGT-3'
Ppia (Cyclophilin)	5'-CTT CGA GCT GTT TGC AGA CAA AGT-3'	5'-AGA TGC CAG GAC CTG TAT GCT-3'